Optica Applicata, Vol. XLIV, No. 4, 2014
DOI: 10.5277/oa140411

Ultraviolet filters for sensors matching biological action spectra

DENIS GAROLI[1], MAURO ALAIBAC[2], MARIA-GUGLIELMINA PELIZZO[1*]

[1]CNR – IFN UOS Padova, via Trasea 7, 35131 Padova, Italy

[2]Unit of Dermatology, University of Padova, via Battisti 206, 35128 Padua, Italy

[*]Corresponding author: pelizzo@dei.unipd.it

A considerable interest is growing worldwide about the photobiological effects of the ultraviolet radiation; in fact, it has been demonstrated that ultraviolet radiation can affect both human health as well as the equilibrium of entire ecosystems. The relative effectiveness of ultraviolet radiation at a particular wavelength in producing a specific biological response is defined by an action spectrum. Broadband radiometers characterized by having a spectral response that matches an action spectrum allow the measure of the effective irradiance associated to an ultraviolet source. In this work we present the designs of interference filters to be used in radiometric heads. Their optimized transmission curve coupled to the spectral response of different ultraviolet photodiodes provides the match of the sensor spectral response with some selected action spectra. Development of instruments for the measurement of the effective solar irradiance is foreseen. The design of interferential filters which transmittance curve was optimized in order to match a target biological action spectrum is here presented.

Keywords: ultraviolet, radiometers, filters, action curve, effective measurements.

1. Introduction

A biological effect of the ultraviolet (UV) radiation is possibly described by an action curve, which is used as a wavelength-dependent weighing factor relative to the spectral UV irradiance; the actual biologically effective irradiance ($W_{\text{eff}}/\text{m}^2$) is then obtained by integrating the weighed spectral irradiance over wavelength. The effective UV dose (in J/m^2) is found by integrating the effective irradiance over the exposure period. In many applications the knowledge of the ultraviolet effective irradiance is fundamental to assess the temporal exposition to an ultraviolet source to accomplish successfully a treatment (for example, a sterilization process or a phototherapy treatment), to limit the exposition to a potential hazardous source, to control the amount of incident UV in photobiological experiments [1].

Irradiance related to a source over the sample depends on the geometry of the set up. Nevertheless many factors contribute to make difficult to predict it, as non-uniformity

of the lamp emission and presence of reflecting/diffusing elements. Therefore, a radiometric head is necessary to evaluate the irradiance.

There are two possible choices for the measurements of the UV effective irradiance: by a scanning instrument represented by a spectro-radiometer or by a broadband instrument, called radiometer. Nowadays there are few commercially available scanning spectro-radiometers that can be used for long term outdoor operation. Nevertheless they do not deliver error free UV measurements mainly because of their limited dynamic range, which, as determined by the action curves, should be of many orders of magnitude. This seriously limits the accuracy of the biological measurements in the ultraviolet and raises the question of whether the biological monitoring cannot be achieved by simpler instruments. These are represented by broadband radiometers. Basically, there are two categories of instruments under this family: the phosphor based Robertson–Berger meter [2] and the interference filter based instruments [3]. Both have fast response and are relatively inexpensive. They can measure one band shaped to a selected action spectrum or a series of narrow bands. Some radiometers are designed in order to have a spectral response that matches a specific action spectrum. This can be accomplished coupling a filter designed to have a proper spectral transmission to a detector with a specific spectral response curve. The operation spectral range of the sensor could be eventually split into two or more ranges by using more than one radiometric head, in order to provide more accurate information; this solution is particularly suitable in the case of the erythema like detector, where the spectral separation into two regions, corresponding to UVB (280–315 nm) and UVA (315–400 nm), could be interesting for particular applications such as sunscreen performance determination [4].

In this work we proposed the design of interferential filters suitable for the realization of radiometric heads having a spectral response equivalent to different biological spectra. Selected action curves are: erythema induction [5], persistent pigment darkening (PPD) [6], DNA damage [7], vitamin D production [8, 9], photokeratitis and photoconjunctivitis [10]. All sensors will be based on similar technology, already presented elsewhere [3]. The radiometer layout consists of a transmission diffuser, an interferential filter and a photodiode detector. The filter is the key element and is specifically designed to make the spectral response of the whole sensor to match the selected action curve. The radiometer integrates a diffuser element to better agree to the cosine law.

2. Action curves and biological effects

Long exposition to sun radiation causes burns, skin aging, erythema and even melanoma cancer. In the European Regulation EN60335-2-27 [1], the toxicity of UV radiation emitting machines for domestic use is discussed and upper-limit exposition effective doses are established. As well as other artificial sources, sun tanning units should be monitored and certified according to the law. There is the necessity to develop a clear measurement procedure to verify sunbed irradiance in metrological laboratories, and

to develop portable instrumentations for the irradiance verification *in situ*. Sunburn is an acute UV caused damage of the skin, manifested by reddening and in some case blistering. The sunburn is a delayed erythema initially characterized by the appearance of "sunburn cells", the depletion of antigen-presenting cells (APC), and the infiltration of the epidermis and dermis by a variety of inflammatory cells, *e.g.*, mast cells, monocytes and lymphocytes. Subsequently the skin responds with hyperproliferation. Sensitivity to sunburn varies based on pigmentation, where lightly pigmented individuals are much more sensitive than heavily pigmented ones. Erythema is induced in a volunteer to test UVB sunscreen protection by sunscreen protection factor (SPF) method. PPD is darkening or tanning of the skin induced by UVA radiation; this physiological effect is also used to carry out an *in vivo* test on sunscreens to measure their UVA protection, similar to the SPF method of measuring UVB light protection.

Instead of measuring erythema or reddening of the skin, the PPD method uses UVA radiation to cause a persistent darkening or tanning of the skin [6]. The PPD action spectrum is very similar to the erythema one, even though limited to the UVA part of the spectrum. DNA is certainly one of the key targets for UV-induced damage in a variety of organisms ranging from bacteria to humans. UV radiation induces two of the most abundant mutagenic and cytotoxic DNA lesions such as cyclobutane pyrimidine dimers (CPDs) and 6–4 photoproducts (6–4 PPs) and their Dewar valence isomers [7]. UV radiation of high intensity can damage the frontmost parts of the eye in a manner of hours or even mere minutes [11]. It can result in inflammation of the cornea (photokeratitis) and of the conjunctiva (photoconjunctivitis). The damage can be felt as a sharp pain in the eyes. Because new cornea and conjunctiva cells constantly re-grow, the damage is reversible [10].

3. Materials and methods

According to the instrument design, the sensor head entrance optics is a Lambertian diffuser, *i.e.*, the equivalent entrance aperture varies with the radiation incidence angle according to the cosine law. Different photodiodes have been previously characterized, as reported elsewhere [12]. The detector based on silicon carbide (SiC) has been evaluated the most appropriate photodiode to be used, since it has a high dynamic range, is very reproducible and inexpensive. In order to match an action spectrum, each filter has been designed to compensate for the photodiode and diffuser spectral response according to the following equation:

$$\frac{\mathrm{AC}(\lambda)}{R_{\mathrm{ph}}(\lambda)R_{\mathrm{diff}}(\lambda)} = R_{\mathrm{filter}}(\lambda) \tag{1}$$

where $\mathrm{AC}(\lambda)$ curve is one of the action curves, $R_{\mathrm{ph}}(\lambda)$ is the photodiode spectral response, $R_{\mathrm{diff}}(\lambda)$ is the diffuser transmission, $R_{\mathrm{filter}}(\lambda)$ is the filter transmission curve target. In this work, a roughened quartz plate with $R_{\mathrm{diff}}(\lambda)$ as reported in [3], has been considered as a diffuser, but the use of a different diffuser material such as Teflon does

not affect the design principle or the quality of the results achievable. Different target curves have been calculated according to Eq. (1), arbitrarily setting their maximum transmission value equal to 100%; in this way, filters with maximized transmission will be optimized.

A commercial software (TFCalc, Software Spectra Inc.) has been used to optimize the design of the filter. For final simulations, optical constants experimentally determined by spectroscopic ellipsometry on a single layer film have been used. The simulation software allows the calculation of a transmission curve of filter structures consisting of up to 5000 layers deposited on a substrate. The radiation incident on the film can be a collimated beam or a cone of rays with a given angular aperture, and the angle of incidence can be varied from 0 to 89.999°. In the case of a cone of rays, the computed transmission corresponds to the average value for the considered angular beam aperture. Simulations have been performed by the use of a white illuminant, *i.e.*, the intensity of the source is uniform over the whole spectral range selected. The software allows the optimization of a filter structure in order to have the transmission curve matching as better as possible the "target curve" (in this case the $R_{\text{filter}}(\lambda)$ curve). Several multilayer designs have been considered by testing different materials and number of layers; by using the optimization software tools, thickness of each layer has been calculated in order to minimize the difference, set according to a merit function, between the target curve and the transmission curve of the filter under design. As materials, SiO_2 and ZrO_2 have been always preferred for the simplicity of deposition. MgF_2 has been proposed in place of SiO_2 only when performances were not satisfied. MgF_2 has a lower refraction index and this allows better optimization of the multilayer structure performance. Even though the deposition of MgF_2 presents some more challenges, the realization of the ZrO_2/MgF_2 has been already achieved [3].

In the following section, the obtained designs will be presented. The quality of the design has been evaluated taking into consideration the response of the complete radiometer, *i.e.*, the designed filter coupled with the SiC photodiode and with the quartz diffuser. The performance evaluation has been based on the following criterion: the response of the complete designed radiometer, computed as the integral over the spectral range of action curve definition (typically 220–400 nm), has been normalized to the nominal value, computed as the integral of the theoretical action curve over the whole spectral range of interest. This corresponds to a typical calibration procedure on a real radiometer. Hence, the quality of the design has been estimated by computing the integral below the response curve over discrete spectral intervals (220–250 nm; 250–280 nm; 280–315 nm; 315–365 nm; 365–400 nm) and comparing the results with the same integral computed below the respective nominal action spectrum. The response curves have been also computed taking into consideration a cone angle of incidence on the system. A 30° cone angle has been used for the computation and the integral below the curve (over the whole spectral range 220–400 nm) has been computed and compared with the previous calculation. Finally, possible tolerances in layer thickness have been evaluated by considering a possible deposition uncertainty of 1 nm. In fact,

the materials required for the presented design can be easily deposited by means of physical vapor deposition methods, such as electron-beam evaporation. In this kind of technologies, a film thickness precision below 1 nm is easy to be obtained. Hence, the integral below the response curves (over the whole spectral range 220–400 nm) will be reported with an error that corresponds to the computation on the same design with layers varied within 1 nm casually. In all the cases, the error is reported in percent.

4. Results and discussion

For each of the action curves selected, two possible designs have been considered, each based on ZrO_2/SiO_2 or ZrO_2/MgF_2 materials couple. The filters designs have been determined in order to match the target curves, as defined by Eq. (1). The number of layers and their thickness for each biological action spectrum related filter are reported

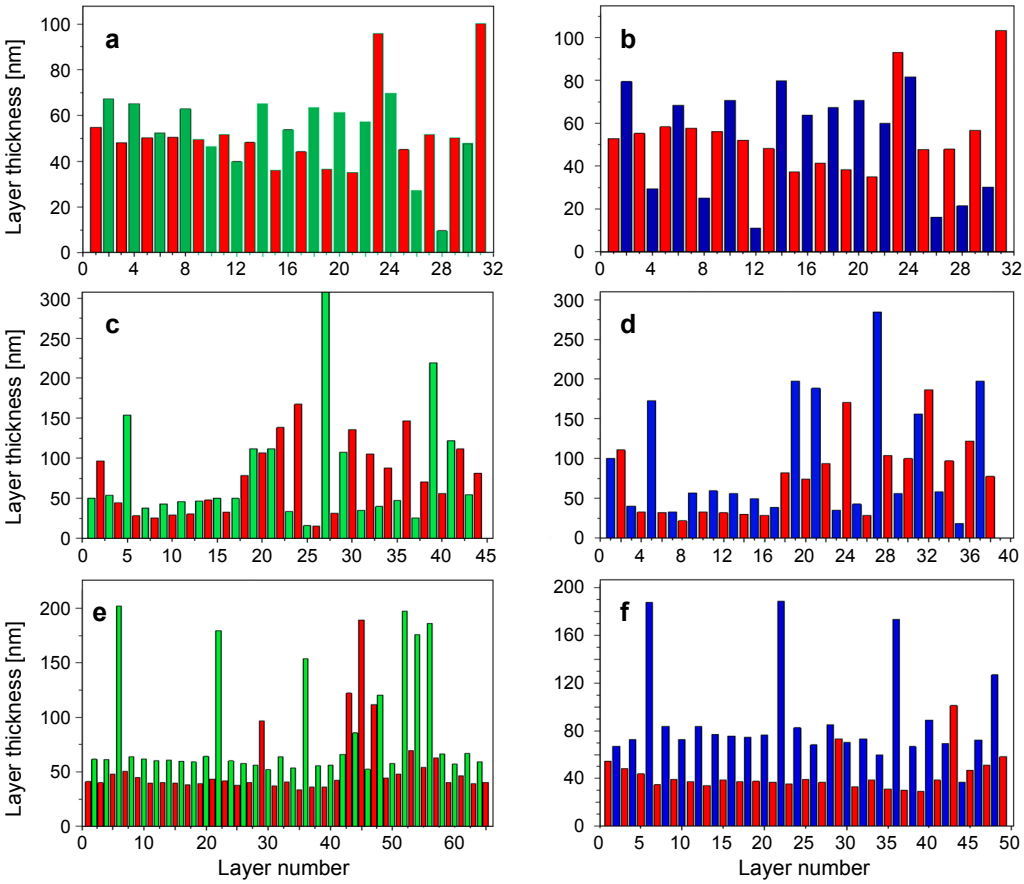

Fig. 1. Layers thicknesses of the proposed filters designs. Erythema filter based on ZrO_2/SiO_2 (**a**); erythema filter based on ZrO_2/MgF_2 (**b**); PPD filter based on ZrO_2/SiO_2 (**c**); PPD filter based on ZrO_2/MgF_2 (**d**); DNA damage filter based on ZrO_2/SiO_2 (**e**); DNA damage filter based on ZrO_2/MgF_2 (**f**).

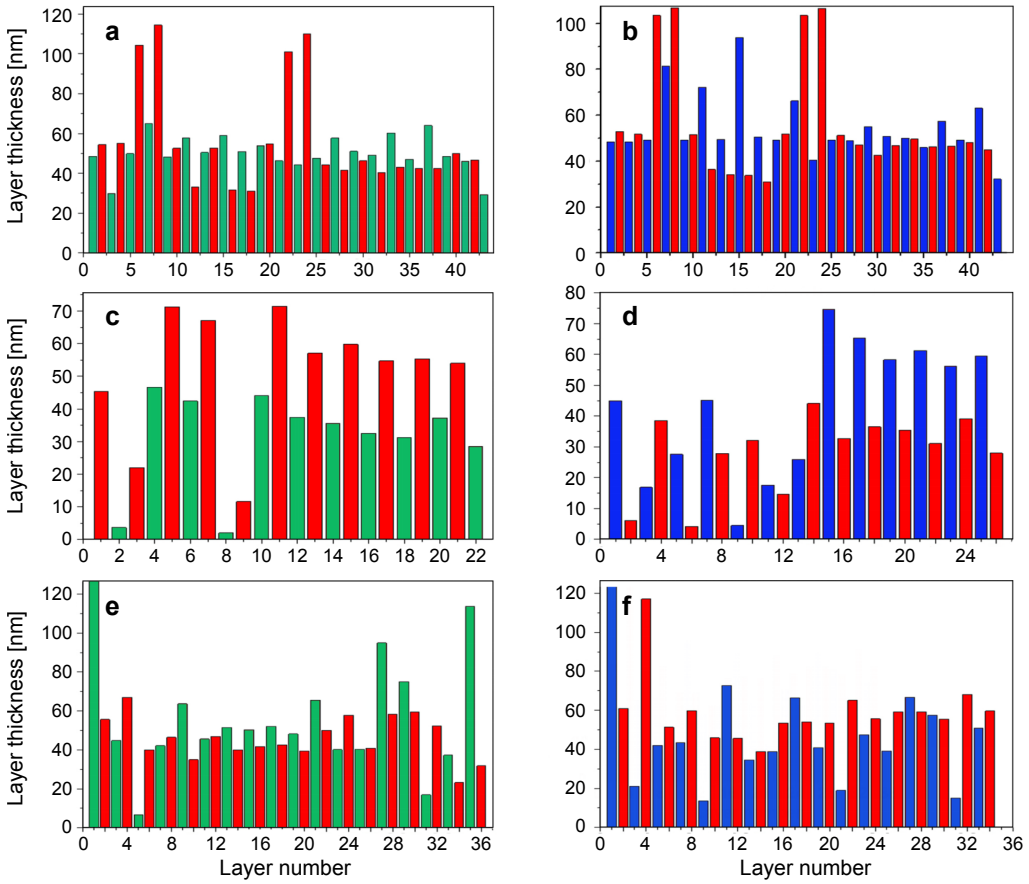

Fig. 2. Layers thicknesses of the proposed filters designs. VitD3 filter based on ZrO_2/SiO_2 (**a**); VitD3 filter based on ZrO_2/MgF_2 (**b**); conjunctivitis filter based on ZrO_2/SiO_2 (**c**); conjunctivitis filter based on ZrO_2/MgF_2 (**d**); keratities filter based on ZrO_2/SiO_2 (**e**); keratities filter based on ZrO_2/MgF_2 (**f**).

in Figs. 1 and 2. In Figure 3 the response curve computed, at normal incidence, by taking into consideration the whole radiometer layout (UV diffuser, interferential filter, UV detector) are reported.

The response curves have been arbitrarily normalized at the theoretical ones by computing the integral below the curves of the whole spectrum of interest. Clearly erythema, PPD, DNA and vitamin D3 (VitD3) action curves are very well matched, while conjunctivitis and keratities action curves are well matched at shorter wavelength, while not so at longer.

Table 1 reports the errors, expressed in percent, computed as illustrated in previous section.

As it can be observed, the errors are below 5% in all the cases in which the computation is done over all the spectral range (case of cone angle and thickness tolerances). Considering a limited spectral range, the errors spans from less than 1% up to 58%.

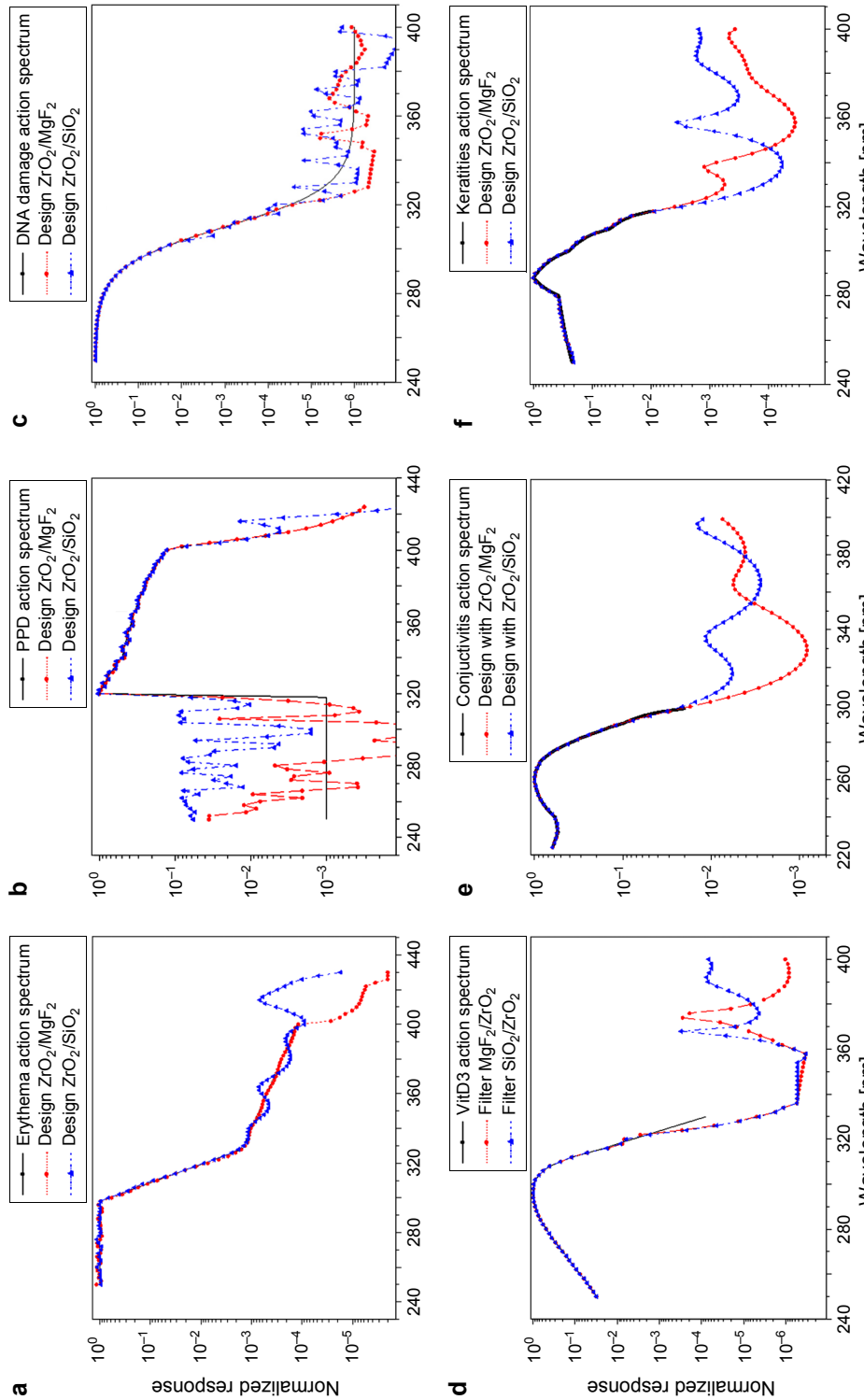

Fig. 3. Nominal action curves and filters+diffuser+photodiode normalized response curves. Direct comparison: erythema action curve (**a**); PPD action curve (**b**); DNA damage action curve (**c**); VitD3 action curve (**d**); conjunctivitis action curve (**e**); and keratities action curve (**f**).

T a b l e 1. Filter design performances (n.d. – not defined).

Design Id.	220–250 nm	250–280 nm	280–315 nm	315–365 nm	365–400 nm	Cone angle (30°)	Thickness tolerance (1 nm)
Erythema ZrO_2/SiO_2	n.d.	0.10	0.26	0.95	1.58	2.62	2.42
Erythema ZrO_2/MgF_2	n.d.	0.04	0.11	0.25	0.47	0.98	2.02
PPD ZrO_2/SiO_2	n.d.	615	340	7.07	8.79	1.15	1.04
PPD ZrO_2/MgF_2	n.d.	472	103	0.64	1.26	4.73	3.49
DNA ZrO_2/SiO_2	n.d.	0.01	0.18	30.13	41.96	4.28	3.21
DNA ZrO_2/MgF_2	n.d.	0.01	0.03	16.03	58.38	2.19	1.13
VitD3 ZrO_2/SiO_2	n.d.	0.50	0.04	10.20	n.d.	2.21	4.91
VitD3 ZrO_2/MgF_2	n.d.	0.50	0.04	10.10	n.d.	3.05	1.27
Conjunctivitis ZrO_2/SiO_2	1.72	1.45	1.65	n.d.	n.d.	2.24	1.68
Conjunctivitis ZrO_2/MgF_2	0.92	0.59	0.73	n.d.	n.d.	1.57	1.27
Keratities ZrO_2/SiO_2	n.d.	1.63	0.9	n.d.	n.d.	3.21	2.65
Keratities ZrO_2/MgF_2	n.d.	1.65	0.8	n.d.	n.d.	3.46	4.15

The higher errors, up to 615%, correspond to the case of PPD in a spectral range where the action curve is very low (250–315 nm). In this region, the proposed radiometer designs give a very low response when compared with the one over 315–400 nm. Hence, these high errors do not reduce the high quality of the response over the whole spectral range. In the Table, some data are not reported (indicated as n.d.), because the action spectrum in these spectral ranges are not defined.

5. Conclusions

The design of different interference filters based on ZrO_2/SiO_2 and ZrO_2/MgF_2 materials couples have been presented. Such filters are coupled with a SiC photodiode and a proper diffuser to realize a portable radiometer able to measure the effective irradiance related to a selected biological action curve. Such instrument is able to perform such measure with an accuracy that is not always possible to be achieved with a spectroradiometer, which usually has a limited dynamic ratio. Such radiometers can be useful in those cases in which a fast but, at a same time, precise measure of effective irradiance is needed.

References

[1] *Specification for safety of household and similar electrical appliances. Particular requirements. Skin exposure to ultraviolet and infrared radiation*, European Regulation EN 60335-2-27, 1997-03; IEC 60335-2-27,1995-05.2, International Electrotechnical Commission, 1995.

[2] Kennedy B.C., Sharp W.E., *A validation study of the Robertson–Berger meter*, Photochemistry and Photobiology **56**(1), 1992, pp. 133–141.

[3] Pelizzo M.G., Garoli D., Nicolosi P., *Realization of a radiometric head for measurements of ultraviolet total erythemal effective irradiance*, Applied Optics **46**(22), 2007, pp. 4977–4984.

[4] Garoli D., Pelizzo M.G., Bernardini B., Nicolosi P., Alaibac M., *Sunscreen tests: correspondence between* in vitro *data and values reported by the manufacturers*, Journal of Dermatological Science **52**(3), 2008, pp. 193–204.

[5] McKinlay A.F., Diffey B.L., *A reference action spectrum for ultraviolet induced erythema in human skin*, CIE Research Note **6**(1), 1987, pp. 17–22.

[6] Moyal D., Chardon A., Kollias N., *Determination of UVA protection factors using the persistent pigment darkening (PPD) as the end point: (Part 1) Calibration of the method*, Photodermatology, Photoimmunology and Photomedicine **16**(6), 2000, pp. 245–249.

[7] Setlow R.B., *The wavelengths in sunlight effective in producing skin cancer: a theoretical analysis*, Proceedings of the National Academy of Sciences of the United States of America **71**(9), 1974, pp. 3363–3366.

[8] MacLaughlin J.A., Anderson R.R., Holick M.F., *Spectral character of sunlight modulates photosynthesis of previtamin D3 and its photoisomers in human skin*, Science **216**(4549), 1982, pp. 1001–1003.

[9] *Action spectrum for the production of previtamin D3 in human skin*, Technical Report, Vol. 174. International Commission on Illumination, CIE, 2006.

[10] Schouten P., Parisi A.V., *Direct comparison between the angular distributions of the erythemal and eye-damaging UV irradiances: a pilot study*, Journal of Photochemistry and Photobiology B: Biology **102**(2), 2011, pp. 146–155.

[11] TREVISAN A., PIOVESAN S., LEONARDI A., BERTOCCO M., NICOLOSI P., PELIZZO M.G., ANGELINI A., *Unusual high exposure to ultraviolet-C radiation*, Photochemistry and Photobiology **82**(4), 2006, pp. 1077–1079.

[12] PELIZZO M.G., CECCHERINI P., GAROLI D., MASUT P., NICOLOSI P., *Absolute spectral response measurements of different photodiodes useful for applications in the UV spectral region*, Proceedings of SPIE **5529**, 2004, pp. 285–293.

Received September 9, 2014
in revised form October 20, 2014